

CHALCOGENIDE NON-CRYSTALLINE SEMICONDUCTORS IN OPTOELECTRONICS

A. M. Andriesh, M. S. Iovu, S. D. Shutov

Center of Optoelectronics, Academy of Sciences of Moldova, 1 Academiei Str.,
MD-2028 Chisinau, Republic of Moldova

The optical, photoelectrical and transport phenomena in chalcogenide vitreous semiconductors are examined taking into account the peculiarities of the energy spectrum. Special attention is paid to photoinduced phenomena in chalcogenide glasses including optical fibers. Several applications of amorphous thin film structures and fibers for optical information storage, integrated optics and various sensors are presented.

(Received May 21, 2002; accepted July 22, 2002)

Keywords: Non-crystalline chalcogenides, Photoinduced phenomena, Optical fibers,
Optoelectronic devices

1. Introduction

It is our great pleasure to dedicate this paper to Professor Stanford R. Ovshinsky, whose contribution to the developing of physics, chemistry and applications of amorphous and disordered materials is highly appreciated in the world. One of the authors of this article, Prof. A. Andriesh, had the honour to meet Mrs. Iris and Mr. Stanford Ovshinsky more than 30 years ago, and from that time till now admired their achievements in the study of amorphous and disordered materials and especially their work in application of a new generation of devices in information and energy fields. It is our conviction that such new materials as chalcogenide glasses and amorphous silicon have received so much attention over the last 30 years mainly due to pioneering activity of ECD Company headed by the famous researcher and engineer Prof. Stanford Ovshinsky.

It is well-known that the scientific and technical progress is based on new phenomena, new materials and new technologies. The development of solid state physics on the basis of quantum mechanics, on one hand, and the obtaining of semiconductor materials of high purity, and especially silicon, on the other hand, have resulted in great achievements in electronics. At present, silicon devices and microelectronic circuits have a very large coverage in micro and nano-electronics. Probably, no other material has so much influenced the civilization as silicon did. However, due to large scale applications of silicon it becomes clear that this material has some limits. It can not assure the effectuation of rapid operations which are characteristic for optical systems. The dramatic increase of the amount of information, characteristic to our epoch, requires the elaboration of systems of processing the optical signals in a parallel mode, that is the registration and processing of signals is produced concomitantly in different channels of information. For these reasons the optoelectronics received a great impulse for development and gained a very large area of applications: from telecommunications till medicine.

The achievements in optoelectronics are based on the materials which could solve these problems. That is why great efforts were made in order to find the corresponding materials. The non-crystalline semiconductors and especially the chalcogenide glassy semiconductors (ChGS) are important materials that are used or can be used in optoelectronics.

Discovered more than 30 years ago by the scientists Prof. B. T. Kolomiets and Prof. N. A. Goriunova, from St.-Petersburg, this class of materials became the subject of scientific research in many laboratories throughout the world. This is due to the fact that these semiconductors supplement

successfully the well-known groups of crystalline semiconductors. While an insignificant change of composition of the crystals is quite sufficient for achieving a sharp change of the physical parameters, the chalcogenide glasses admit smooth change of properties even in cases of considerable changes of the composition of the alloy.

Many electronic processes in crystals are controlled by the redistribution of charge carriers over separate discrete local levels. The chalcogenide semiconductors show a quasi-continuous distribution of localized states, which generates peculiarities of electronic processes, in particular, in transport, in optical and photoelectric processes. In ChGS the mobility of charge carriers may differ from the mobility in crystals by several orders of magnitude.

While the crystals having rigid structures do not permit removing of atoms from their fixed position in the network, the chalcogenide glasses, as well as other disordered materials having a more mobile structure, allow for changing the position of neighboring atoms under very small energetic fluence by means of optical, X-ray radiation or electron beam. Comparing the properties of crystals and of glasses, the enumeration of these peculiarities of the chalcogenide glasses may be continued, but probably, even those mentioned above are quite sufficient for stressing the originality of the properties of chalcogenide glasses, allowing us to propose the above-mentioned class of materials for wide applications.

We will confine ourselves to present only short information concerning the peculiarities of energy spectrum, transport phenomena, photoelectrical and optical properties, especially photoinduced phenomena, some results of application of this group of materials in optoelectronics, which were for a long time in the sphere of interests in the Institute of Applied Physics of the Academy of Sciences of Moldova.

2. Peculiarities of the structure and distribution of electron states in ChGS

2.1. Peculiarities of structure

It is well-known that the crystalline solid state is characterized by strict order in the position of atoms even at large atomic distances. This is not the case in non-crystalline solids, for example, in ChGS. These materials could be characterized by short range order (SRO) and partially by intermediate range order (IRO). That means that after changing the crystalline state of a crystal in vitreous or amorphous state the shortest distance between neighboring atoms is almost the same as in the crystal, may be, only with small distortion, which certainly leads to destroying of the long range order (LRO). For example, the first atomic coordination in the crystals and glasses of As_2S_3 and As_2Se_3 are almost the same [1]. Of course, this is not characteristic for all materials. The germanate glasses (Ge_xCh_{1-x}) are a typical example of different SRO in crystals and glasses of the same composition [2,3].

The distortion of SRO while the crystal is transforming in glass even in the case when such distortion is quite small as in the case of As_2S_3 and As_2Se_3 leads to drastic change of energy spectrum, especially in the forbidden energy band. Instead of discrete energy levels of impurity states the quasicontinuous distribution of states is observed. The possible sense of such distribution of electron states will be commented further.

It is necessary to note that in the process of study of the structure and optical properties of glasses an intermediate order in the location of atoms was observed. For the characterization of the existence of the order in the position of the atoms out of the sphere of nearest neighbors, new terms were introduced, such as IRO [4] and MRO [5]. It is very important that IRO is very sensitive to external radiation and can be manifested through the so called photostructural changes.

The influence of metal dopants (Sn, Dy, Sm and Mn) on the structure of vitreous As_2S_3 and As_2Se_3 studied by X-ray diffraction method [6] appears primarily in the medium-range ordering of the glassy network. A significant shift of the first sharp diffraction peak (FSDP) from the position corresponding to the pure As_2S_3 and As_2Se_3 glasses was observed in the diffraction curves (Fig. 1). The direction of the shift depends on the type of the metal introduced in the ChGS matrix. Fig. 2 shows the plot of the interlayer distance shift $\Delta d/d(\%)$ versus the per cent of ionicity in the metal-

selenium (Me-Se) bond. This relation indicates the importance of the Me-Se interaction for the MRO in glass.

The As_2Se_3 layers are locally distorted by the insertion of the metal atoms that bond to Se. A high covalence of the Me-Se bond gives rise to strong directional bonds and the layers become more rigid while high metal ionicity diminishes the stiffness of the layers. It was shown that Sm and Dy play the role of network modifier, while Mn and Sn play the role of network former of the glass lattice. The disordered layers are stiffed by the insertion of the atoms with directional bonds. In this case the interlayer distance is increased due to the increase of the effective thickness of the layers. The effect of the low metal ion contents on the structure of As_2S_3 and As_2Se_3 glasses can be explained by co-operative effects.

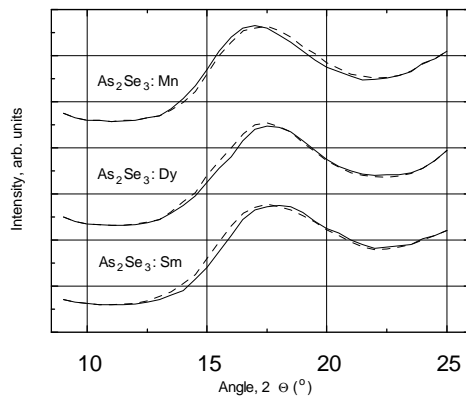


Fig. 1. The X-ray curves in the region of the FSDP of the metal doped As_2Se_3 glass.
--- As_2Se_3 :0.1 at.% Me; — As_2Se_3 :0.5 at.% Me

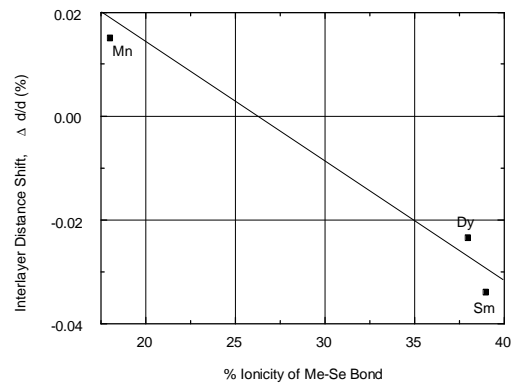


Fig. 2. The relation between the shift of the interlayer distance in As_2Se_3 induced by doping with various metals and the degree of ionicity of the Me-Se bond.

2.2. Peculiarities of distribution of localized electron states

Mott and Davis [7] proposed the first models of distribution of localized states in non-crystalline solids. The key point of these models is the quasi-continuous distribution of localized states in the forbidden gap which arise due to structural disorder in non-crystalline solids. According to Gubanov [8], the absence of the long range order (LRO) in the distribution of atoms leads to the blurring of the conductive band edges and to the appearance of fluctuations levels. Cohen, Fritzsche and Ovshinsky [9] have proposed the model of tail density of electron states which are spreadly in the forbidden gap. In dependence of the degree of ordering of the semiconductor the tail density of states is distributed near the edges of allowed bands or is spread deeply in the forbidden gap up to their mutual overlap. In the models of Mott and Davis [7] besides the tails of allowed bands near the middle of the forbidden gap the existence of rather narrow band (~ 0.1 eV) of localized states is supposed. According to Kolomiets [10] in vitreous semiconductors on the background of monotonous level distribution some bands with heightened state density can be observed. Marshall and Owen [11] localized the bands with higher density of localized states both in the upper and lower half of the forbidden gap. There was demonstrated by Bonch-Bruevich [12] that in the forbidden gap of the disordered semiconductor the peaks of density of localized states are possible, conditioned by the presence of impurities or other defects, which with some assumptions can be named discrete localized levels. The nature of localized states in vitreous semiconductors is still not enough clear. Several papers these states were connected with the presence of defects. The first paper related to this problem is the publication of Street and Mott [13] where the localized states given by broken bonds were analyzed. These states depending on the engaged electron bonds correspond to the neutral, positive or negative charged centers.

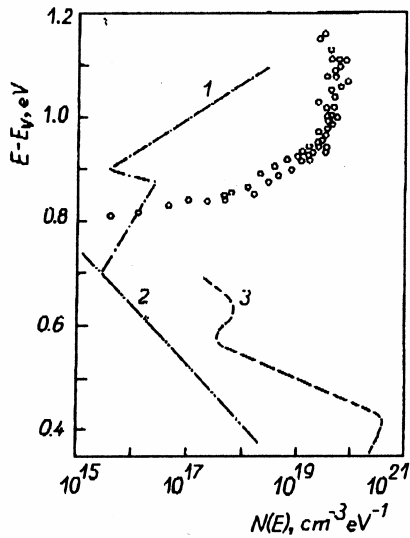


Fig. 3. Sketch of the density of localized states distribution in the gap of As_2Se_3 , 1 – according [14], 2 – according D. Monroe, M. A. Kastner, *Phys. Rev.* **B33**, 8881 (1986), 3 – according R. P. Barclay, J. M. Marshall, C. Main, *J. Non - Cryst. Solids*, **77&78**, 1269 (1985), and 4 – according [15].

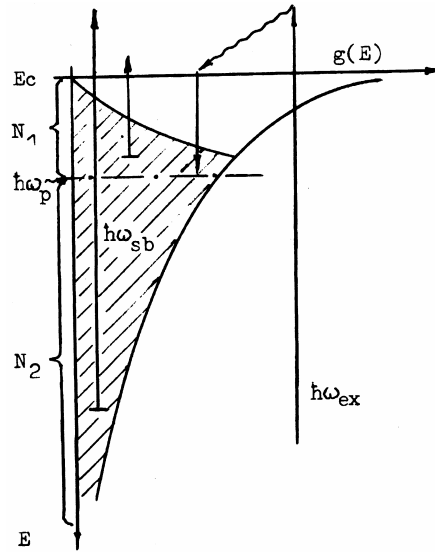


Fig. 4. The steady-state excess carrier distribution in the exponential tail of localized states.

We applied many experimental methods while the aim to obtain the adequate distribution of localized states in the forbidden gap: thermostimulated currents, thermostimulated electrical depolarization, spectral distribution and kinetics of photoconductivity, transport phenomena, optical absorption and photoinduced absorption etc. On the basis of these experiments we not only confirmed the quasi-continuous distribution of localized states in the forbidden gap with some portions with higher density but even were able to calculate in some energy range the precise parameters of the energy distribution. For example, using the charging and discharging characteristics of Metal-ChGS-Semiconductor-Dielectric-Semiconductor structure ($\text{Me-As}_2\text{S}_3(\text{As}_2\text{Se}_3)\text{-SiO}_2\text{-Si}$) the authors [14] determined that the energy distribution of the filled traps is quasi-continuous with an asymmetric maximum in the energy range of 0.70-0.90 eV for As_2Se_3 and 0.85-1.05 eV for As_2S_3 , respectively (Fig. 3). By studying the change with time of the transient capacitance of the space charge region at a Schottky barrier due to thermal relaxation of localized centers preliminary filled by a pulse of zero bias, the authors [15] determined the density of states distribution in the upper half of the gap of As_2Se_3 in the interval of 0.35 eV above the Fermi level.

3. Transport phenomena

The transport phenomena in ChGS are determined by the spectrum of energy distribution of localized states (Fig.4). The existence of high concentration of localized states in ChGS causes a capturing of free carriers by quasi-continuously distributed states in the forbidden gap. So, the transport of the carriers occurs when the carriers are excited from traps thermally or by light. But these carriers take part in conductance only during a short period of time, and afterwards they are captured again. When carriers are trapped they do not participate to conductivity. Of course, even in the case of trapped carriers they can participate to the conductivity by hopping process, but this kind of conductivity is small in the case of not very high concentrations of traps near the Fermi level.

The distribution of traps in a large energy range leads to the distribution of escape times of carriers from traps, which depends on energy depth of localized states that leads to the dispersion type of the escaping times. That is why such type of transport is named dispersive transport. For increasing of current one injects the pulse of carriers through contact or by light excitation. In this case the

transport current has not the plato characteristic for quasi-equilibrium transport as it shown in Fig. 5. However, it was proved that one can observe in the logarithmic scale the transition from one type of the curve $j(t) \sim t^{-(1-\alpha)}$ to another $j(t) \sim t^{-(1+\alpha)}$ with the transition point being dependent on the parameters of the energy distribution of traps, temperature T and the E/L ratio, where E – is the applied electric field, and L – is the thickness of the sample [16]. The dependences were calculated analytically by the authors from [17] and were used for obtaining the parameters of the energy distribution of localized states. For example, for exponential distribution of traps the dispersion parameter α is described by eqn. $1/\alpha \sim E_{\text{eff}}/kT^*$, where E_{eff} corresponds to the parameter of energy distribution of the localized states. The parameter E_{eff} can be changed by changing the composition of the ChGS, by thermal treatment or by doping. As it was shown by the authors from [18], in the case of introducing Dy in the glass, one can observe the drastic change of the dark conductivity and photoconductivity. It can be seen from the temperature dependence of the conductivity of As_2Se_3 (Fig. 6.) and also from the spectral distribution of photoconductivity (Fig.7). The activation energy, E_a , dropped down from 0.85 eV for As_2Se_3 to 0.5 eV for $\text{As}_2\text{Se}_3+0.5$ at.% Dy and a wide impurity band located around 1.05 eV appeared in the photoconductivity spectrum. In accordance with conductivity results this absorption band induces a group of deep traps by doping with Dy, which increase the recombination rate.

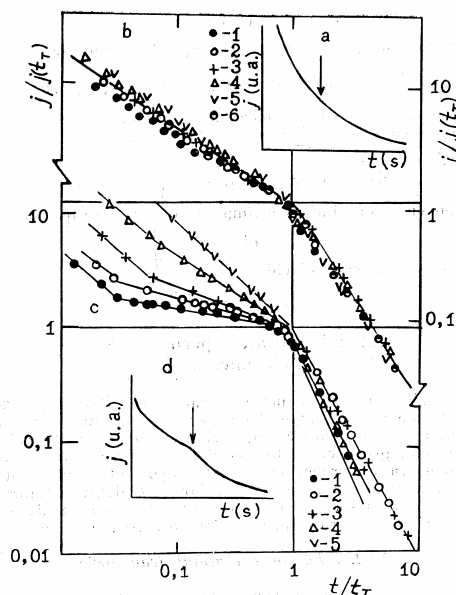


Fig. 5. Normalized photocurrent transients in linear (a,d) and logarithmic (b,c) units for $T = 65$ °C (a,b) and $T=165$ °C (c,d). The parameters of the curves are:
a) $L=1.5$ μm , $E=2 \cdot 10^5$ V/cm;
b) $L=1.5$ μm , E : V/cm: 10^5 (1), $2 \cdot 10^5$ (2), $4 \cdot 10^5$ (3), $8 \cdot 10^5$ (4), 10^5 (6);
c) $L=6.3$ μm , E : V/cm: 10^4 (1), $4 \cdot 10^4$ (2), $8 \cdot 10^4$ (3), $2 \cdot 10^5$ (4), $4 \cdot 10^5$ (5);
d) $L=1.5$ μm , $E=10^5$ V/cm;

High concentration of traps particularly influences the kinetics of photoconductivity delaying the process of reaching of steady-state value or the process of relaxation of the photocurrent after stopping the illumination [19]. This process can be explained in terms of the model of long-living ordered electron structure with large electron-hole distance survive, leading to the ordered structure of the ChGS. This causes the long living conductivity [20].

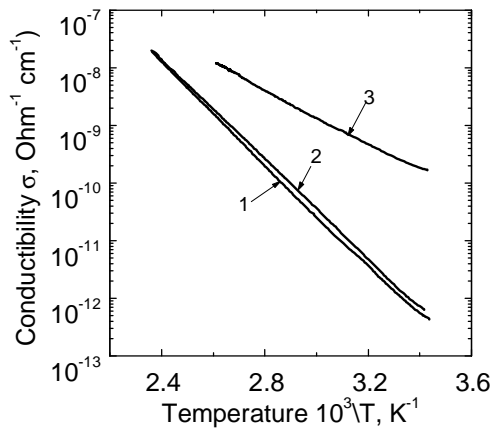


Fig. 6. The temperature dependence of conductivity for As_2Se_3 (1), $\text{As}_2\text{Se}_3 + 0.1$ at.% Dy (2) and $\text{As}_2\text{Se}_3 + 0.5$ at.% Dy.

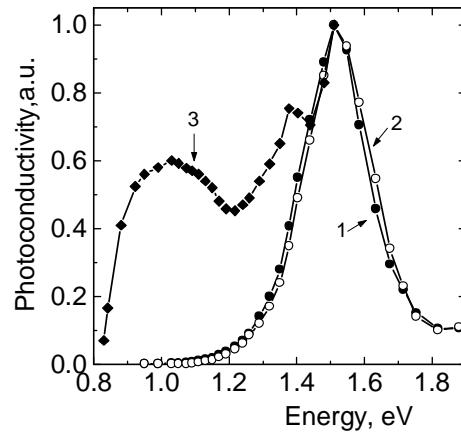


Fig. 7. The spectral distribution of photoconductivity for As_2Se_3 (1), $\text{As}_2\text{Se}_3 + 0.1$ at.% Dy (2) and $\text{As}_2\text{Se}_3 + 0.5$ at.% Dy.

4. Optical properties

4.1. Absorption edge

The study of the absorption edge in chalcogenide glasses is of great interest because optical illumination and other kinds of irradiation strongly affect the position of the absorption edge. For the study of these phenomena it is convenient to use such materials as As-S, As-Se, Ge-S, Ge-Se, that can be obtained in crystalline and non-crystalline forms, and ChGS doped with different metal impurities.

The absorption edge of these materials is situated in the visible range of the spectrum and consists of three parts [21]:

- The first part in the region of high absorption coefficients, $\alpha > 10^4$, cm^{-1} can be described by a quadratic dependence:

$$\alpha = [A(T)/h\nu][h\nu - E_g(T)]^2, \quad (1)$$

where E_g is the optical gap, which in the case of As_2S_3 is equal to 2.35 – 2.38 eV.

- In the range of the absorption coefficients $\alpha \approx 1-3 \times 10^3$ cm^{-1} (Urbach tail) the optical absorption follows the exponential function:

$$\alpha = \alpha_0 \exp\{-[E_0(T) - h\nu]/\Delta_1\} \quad (2)$$

for $h\nu < E_0$, where E_0 almost coincides with E_g and Δ_1 is equal to 0.05 eV. While the temperature T is decreased the edge moves to lower energies with the temperature coefficient $\sim 1.6 \times 10^{-3}$ eV/°C.

- In the range of the absorption coefficients $\alpha < 1$ cm^{-1} the absorption coefficient is described by the exponential function, too:

$$\alpha \sim \exp(h\nu/\Delta_2), \quad (3)$$

but the parameter Δ_2 is larger and its value depends very much on the conditions of the synthesis and on impurity concentration.

This type of the absorption edge was observed in all studied compositions of ChGS. The nature of the absorption edge in non-crystalline solids was thoroughly studied by many authors and is connected with structural disorder. The structural disorder consists of two parts: the disorder of the thermal nature – which is characteristic of the crystals, and the disorder of the atomic structure which is characteristic of the non-crystalline solids [22]. Such an interpretation of the absorption edge in non-crystalline solids enables us to study the structure of such materials by studying the optical properties.

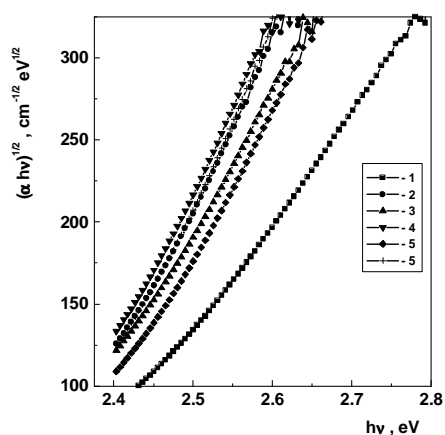


Fig. 8. Absorption spectra of thin films; As_2S_3 (1), $\text{As}_2\text{S}_3+0.1$ at.% Dy (2), $\text{As}_2\text{S}_3+0.1$ at.% Sm (3), $\text{As}_2\text{S}_3+0.5$ at. % Sm (4), $\text{As}_2\text{S}_3+0.1$ at. % Mn (5) and $\text{As}_2\text{S}_3+0.5$ at.% Mn (6).

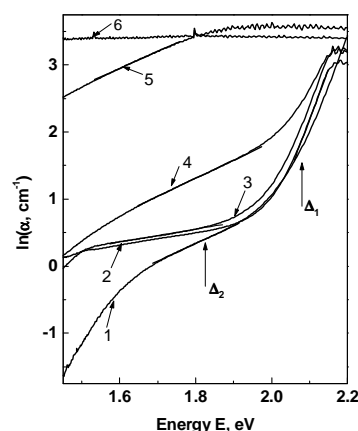


Fig. 9. The absorption spectra of bulk glasses; As_2S_3 (1), $\text{As}_2\text{S}_3+0.1$ at.%Sm (2), $\text{As}_2\text{S}_3+0.5$ at.%Sm (3), $\text{As}_2\text{S}_3+0.1$ at. % Dy (4), $\text{As}_2\text{S}_3+0.1$ at. % Mn (5) and $\text{As}_2\text{S}_3+0.5$ at.%Mn (6).

The optical absorption edge spectra of As_2S_3 glass doped with rare earth (Dy and Sm) and transition (Mn) luminescent impurities in the high absorption region is presented in Fig.8. The optical gap E_g determined by extrapolation of the straight-line portions of the $(\alpha \cdot hv)^{1/2}$ vs. (hv) graphs was found to be 2.34 eV for As_2S_3 . Doping of As_2S_3 glass with metal impurities decreases E_g (Table 1), the new optical gap value being dependent on the nature and concentration of the metal ion dopant [23].

The absorption spectra in the Urbach region ($\alpha \approx 1 \div 10^3 \text{ cm}^{-1}$) and in the region of weak absorption ($\alpha < 1 \text{ cm}^{-1}$) for As_2S_3 doped glasses are shown in Fig. 9. The Δ_1 value for As_2S_3 is $\Delta_1=0.056$ eV, whereas for As_2S_3 doped with Dy and Sm Δ_1 is found to be somewhat higher (Table 1). For As_2S_3 doped with Mn the absorption coefficient in this region is very high, and almost frequency independent for the 0.5 at. % Mn glass. The broadening of the Urbach tail is caused probably by the formation of new impurity metal-based structural units, which add compositional disorder to the existing structural disorder. This effect is possibly responsible for the drastic increase of absorption in samples doped with Mn, where new Mn-based structural units with lower optical threshold energy may be formed resulting in the decrease of the mean value of the gap as in the case of alloys.

Table 1. The optical band gap, E_g , and the parameters Δ_1 , Δ_2 values of As_2S_3 doped glasses.

Glass composition	E_g , eV	Δ_1 , eV	Δ_2 , eV
As_2S_3	2.34	0.056	0.31
$\text{As}_2\text{S}_3+0.1$ at.% Dy	2.29	0.11	0.31
$\text{As}_2\text{S}_3+0.1$ at.% Sm	2.30	0.07	1.02
$\text{As}_2\text{S}_3+0.5$ at.% Sm	2.29	0.07	1.02
$\text{As}_2\text{S}_3+0.1$ at.% Mn	2.32	-	0.31
$\text{As}_2\text{S}_3+0.5$ at.% Mn	2.30	-	-

The value of Δ_2 for vitreous As_2S_3 ($\Delta_2 \approx 0.31$ eV) is strongly affected by doping (Table 1). The weak absorption tails in chalcogenide glasses may be attributed to additional states created by defects and/or impurities, or to the increase in the average amplitude of the internal electric fields produced by the introduction of additional charged centres. The latter interpretation can be applied to the present case since Sm/Dy and Mn dopants enter the host glass as three (Sm^{3+} , Dy^{3+}) - and two-fold (Mn^{2+}) charged ions, respectively. .

The metal impurity induced changes in the intermediate order of amorphous matrix dependent on the type of impurity. This particular fact presents special interest as regards the novel photodarkening model of Shimakawa et al. [24], which links the photodarkening (and photoexpansion) with changes in intermediate ordering that restrict mutual slip motion of the network

clusters. We have investigated the photodarkening effect and its kinetics in amorphous As_2Se_3 chalcogenide films doped with 0.5 at.% of metals Sn, Mn and rare earths Sm and Dy [25].

All $\text{As}_2\text{Se}_3:\text{Me}$ films underwent typical photodarkening under illumination. Red shift of the transmission edge after exposition was clearly observed as well as the corresponding decrease of the transmission in agreement with the published data. Relaxation of optical transmission $T(t)/T(0)$ of the $\text{As}_2\text{Se}_3:\text{Me}$ films in dependence on the exposure time t is shown in Fig.10 for untreated (u) and annealed (a) films, respectively, and in Fig.11 for different concentration of metal (Pr) impurity. At a constant light intensity the presented dependencies characterize the reduction of film transmittance with the increase of the dose of absorbed photons. Note, that 0.5 at.% of metal impurity significantly weakens the photodarkening effect, especially for Sn and Dy. The heat treatment and metal impurity reduce photodarkening and the degree of reduction depends on the sort of impurity. The relaxation process may be described by a stretched exponential with the dispersive parameter $0.5 < \alpha < 1$ and time constant increasing with embedding of impurity or thermal annealing. Doping of amorphous chalcogenide films by metals assists in stabilizing the glassy matrix with respect to light exposure and thermal treatment.

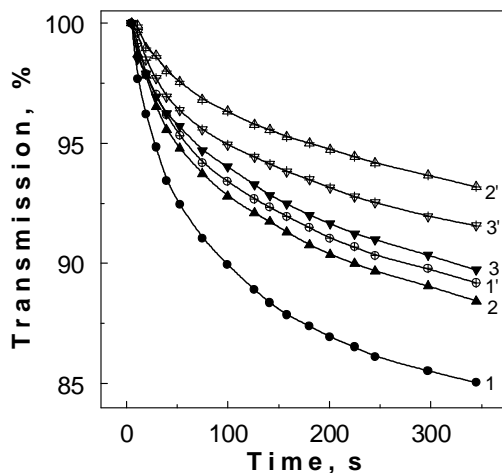


Fig. 10. Photodarkening kinetics of $\text{As}_{40}\text{Se}_{60}:\text{Me}$ films with exposure time for untreated (1,2,3) and annealed at $T=100^\circ\text{C}$ ($1',2',3'$) samples: 1,1' - $\text{As}_{40}\text{Se}_{60}$; 2,2' - $\text{As}_{40}\text{Se}_{60}+0.5\%$ Sn; 3,3' - $\text{As}_{40}\text{Se}_{60}+0.5\%$ Dy. Lines show fitting of the experimental points with the stretched exponential.

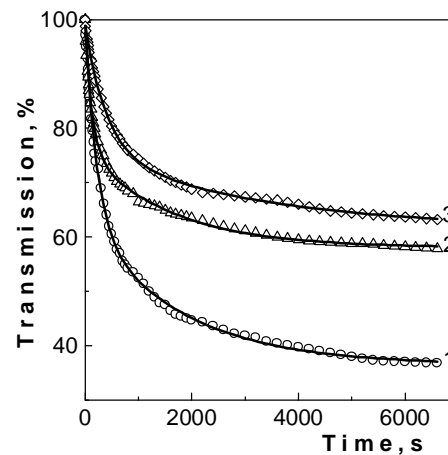


Fig. 11. Photodarkening kinetics of $\text{As}_{40}\text{Se}_{60}$ (1), $\text{As}_{40}\text{Se}_{60}+0.5\%$ Pr (2), and $\text{As}_{40}\text{Se}_{60}+1.0\%$ Pr (3) films with exposure time for untreated samples. Lines show fitting of the experimental points with the stretched exponential.

4.2. Photoinduced absorption on the basis of electron processes

As it was mentioned above the structure disorder in non-crystalline solids causes a quasicontinuous distributing of the localized states in the forbidden gap. While the ChGS samples are excited by the light with the energy of $h\nu > E_g$ non-equilibrium carriers appearing in the free bands are very quickly captured by the localized states and participate in the photoinduced absorption (PA) at the energies of $E < E_g$ (Fig.4).

As it was confirmed by many experiments, the characteristic time of the photoinduced processes is spread in a wide range of values from $\sim 10^{-12}$ to 10^3 s. The long life photoinduced processes are connected with the change of the physico-chemical properties of the ChGS and are termed in the scientific literature as photostructural transformations. The photostructural transformations are observed as a rule in the ChGS thin films and they are accompanied by the shift of the absorption edge to the lower energy, by the decrease of the steepness of the edge and by the change of the optical parameters while the intensity of the exciting light was very low, of the order $\sim 10^{-6} - 10^2 \text{ W/cm}^2$ [21].

The use of fiber samples rather than film or bulk samples enabled us to better observe the small changes in mid-gap optical absorption at low intensity of exciting light because of the longer optical path of the probing light in the fiber. The probing light with photon energy $h\nu < E_g$ from the mid-gap energy range was launched into the input face of the fiber. In the output in the fiber the intensity of the probing light transmitted through the fiber was measured. When the fiber side surface is illuminated with continuous bandgap light the intensity of the probing light at the output of the fiber decreases from its initial value (in the dark) I_o to a new one I . The photoinduced absorption coefficient $\Delta\alpha$ is determined as follows:

$$\Delta\alpha = L^{-1} \ln(I_o/I),$$

where L is the length of the illuminated segment of the fiber. It should be noted that the intensity of the probing light in PA in our experiments was chosen to be so weak that it did not cause any significant change in the PA coefficient. The main feature of the PA in our experiments is a full restoration of the minimal optical transmittance after stopping the illumination. The restoration rate depends on the illumination conditions and the ChGS composition. The spectral distribution of the PA coefficient measured in the energy range of probing light 0.6-1.9 eV is presented in Fig. 12.

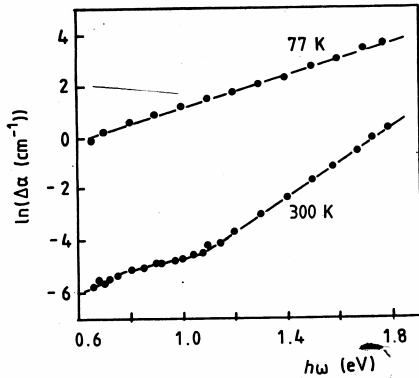


Fig. 12. Spectral distribution of PA steady-state-coefficient $\Delta\alpha$ in As_2S_3 fibers after irradiation with Ar-laser light ($\lambda_{exc} = 0.46 - 0.52 \mu\text{m}$). The intensity of the exciting light $P_{exc} = 10 \text{ mW/cm}^2$.

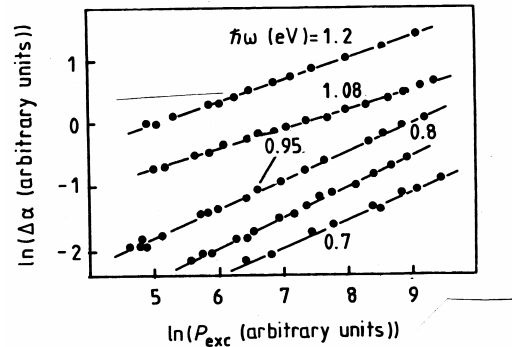


Fig. 13. Intensity dependence of the PA steady-state-coefficient $\Delta\alpha$ in As_2S_3 fibers for various probing light photon energies at room temperature. The wavelength of the exciting light $\lambda_{exc} = 0.35 - 0.75 \mu\text{m}$.

We note the exponential character of the $\Delta\alpha$ vs. $h\nu$ dependence for a rather large energy range. Illumination of the fiber at a low temperature ($T=77 \text{ K}$) leads to a significant increase of PA with respect to room temperature illumination [26]. The intensity dependence of the PA $\Delta\alpha \sim P_{exc}^n$, when the intensity of the exciting light (P_{exc}) is varied by about four orders of magnitude ($10^{-6} - 10^{-2} \text{ W/cm}^2$). The value of n changes with probing light photon energy in the range 0.3 - 0.5 (Fig. 13).

The experimental results can be interpreted in terms of the model with carriers multiple trapping in localized states (Fig. 4), distributed continuously in the forbidden gap [26]. Illumination of the fiber with the bandgap light leads to excitation of non-bonding electron states and injection of excess carriers into the conduction band. Shortly after excitation the electrons are captured by the tail states proportionally to their density, since the capture coefficient is supposed to be the same for different values of trap energy, E . The appearance of excess carriers on the localized states in the gap leads to an additional absorption of probing light in a wide energy range $h\nu < E_g$. The fact that the dependence of PA has a power law character following the square-root function confirms that the carriers excited in the process of PA as well as the carriers participating in photoconductivity recombine according to bimolecular mechanism. As it was shown in paper [27] this can be used for determining the magnitude of bimolecular coefficient from PA data and to calculate on this basis the magnitude of drift mobility. This is very important in the case of high resistivity semiconductors such as As_2S_3 and As_2Se_3 glasses.

4.3. Photoinduced absorption on the basis of phase change

There exist ChGS which have two or more distinct atomic structural states characterized by different amounts of disorder. An energy barrier separates the structural states thereby providing the temporal stability required for a memory devices. The change of atomic configuration can be realized by exposure to a laser beam, electron beam or electrical field. By the way, laser beam can be used not only for recording but also for erasing and rewriting processes each of these processes being going on at the different levels of intensity of the beam. Selecting the composition of the ChGS it is possible to produce transformation between amorphous and crystalline structural system GeTe and Sb_2Te_3 [28]. The phase change materials were successfully used for optical memory disks with 650 Mb capacity and the next product to be introduced will be 2.6 Gb DVD-RAM disk [28].

In explaining the process of Ag-migration in Ag-As(Ge)-S(Se) glasses the authors [29] proposed the mechanism of photo- and electron- induced chemical modifications. As it was shown, light illumination and electron beams accelerated at low voltages can induce Ag-gathering effects. The mechanism is assumed to be caused by intrinsic electric fields built up by photoexcited carriers and by electrons [30]. Studying the physico-mechanical and structural modifications in $Ge_xAs_{40-x}S_{60}$ amorphous films induced by UV-light irradiation the authors [31] observed that irradiation is accompanied with significant release of sulphur which leads to a giant film contraction. By X-ray diffraction studies a significant structural modification induced in pure and tin-doped AsSe thin films by UV irradiation as detected [32]. It was shown that long time UV ($\lambda=336$ nm) irradiation in air induced the formation at the surface of the films of As_2O_3 (arsenolite) layer. Tin has a stabilizing effect against the transformations of the AsSe films with a maximum effect for ~ 3 at.% Sn. The structural modifications of the AsSe films as a function of the doping and the resistance of the film against UV irradiation were explained in the frame of the Shimakawa's model [24].

4.4. Optical hysteresis and nonlinear absorption laser pulses in ChGS

The interest to the study of the nonlinear propagation peculiarities of the laser radiation in non-crystalline semiconductors is due not only to the new fundamental physical mechanisms present in these materials, which can appear in the strong fields of the laser pumping, but also to the wide spectrum of possible applications in the optoelectronic devices and photonic switching. The promising effects are the optical bistability and optical hysteresis, on the basis of which it is possible to produce fast-acting, all-optical switching and logical elements. In recent years a variety of both passive (fibers, planar waveguides, lenses, gratings) and active (nonlinear devices, mainly based on Fabry-Perot interference, optical bistability and optical hysteresis) elements have been demonstrated [21]. For this reason the nonlinear interaction of laser pulses with ChGS thin films ($L=0.2 - 5.0$ μm) samples of As_2S_3 , As_2Se_3 , AsSe, GeS₂, $As_{22}S_{33}Ge_{45}$ and α -Si:H were investigated. It was shown, that when the input light (with $h\nu > E_g$) pulse intensity was relatively low, the transmission of ChGS thin films decreased according to the usual linear light absorption coefficient for the given wavelength. However, the increase of the incident light intensity over definite threshold values (I_o) leads to a nonlinear character of the light transmission by the ChGS thin films [21]. Fig.14 shows the experimental and the calculated hysteresis dependencies of the pulse intensity, passed through an AsSe film ($L = 0.6 \mu m$), versus the corresponding intensity value at the input, for 7 ns laser pulse duration [33]. The characteristic value of the threshold light intensity depends on the ChGS film composition, wavelength of excitation, temperature and the laser pulse duration.

As a result of the nonlinear light absorption a change of time profile of the laser pulses is observed which leads to a hysteresis dependence of the output light intensity on the corresponding value of the input intensity. Nonlinear absorption in chalcogenide glasses was observed even in femtosecond range that is due to either intraband or interband transitions. A new mechanism of a nonlinear light absorption in ChGS, taking into account the interaction with non-equilibrium phonons and localized vibrational modes was proposed.

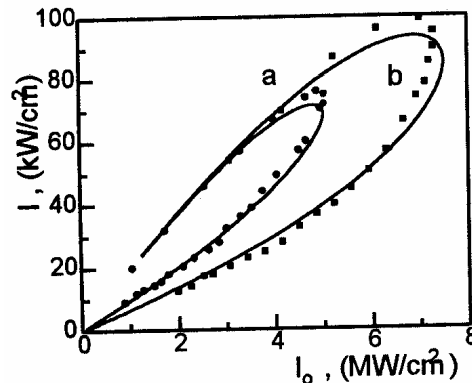


Fig. 14. Experimental (symbols) and calculated dependencies of transmitted light intensity versus input one (I_o). Pulse peak intensity: 5.0 (a) and 7.5 MW/cm² (b).

5. Devices based on ChGS

Many devices can be developed on the base of ChGS, which can change their electrophysical and optical parameters under applied electrical field, exposition to light electron beam, X-ray irradiation etc. At the same time they manifest resistance to nuclear radiation. Besides that, ChGS could be obtained using very simple technologies and in many cases (but not in all cases) they do not need very high purity. It is possible to produce industrially electrical switches, xerographic and thermoplastic media, photoresistant and holographic media, optical filters, optical sensors, thin films waveguides, nonlinear elements, etc.

In 60's a great attention was paid to threshold switching elements which were able under the pulse of voltage to pass from the state OFF with a very high resistivity to the state ON with low resistivity [28]. The industrial technology was started by S. R. Ovshinsky who named his optimized element as ovonic threshold switching [28, 34]. The switching acts in the very short time less than 10 nanoseconds. A great success was utilization of ChGS thin films as target in vidicon image tube (for TV camera). Now we will present some optoelectronic devices developed in our Center of Optoelectronics.

5.1. Registration media and holographic information technologies

The progress of science and engineering presents new requirements to holographic recording media: diminishing of the recording time, high stability and possibility of recording over large areas. These requirements are partially satisfied by registration media based on chalcogenide glassy semiconductors (ChGS). At the same time the modern development of the holographic techniques requires recording holograms and reconstruction of images in real time. New recording structures based on ChGS and new methods of holographic recording were proposed. The change of the surface relief in the "sandwich" amorphous thin film structures under simultaneous action of the illumination and applied electric field was established by several authors [35-38]. The nature of the electrostimulated and photoinduced surface microdeformations in Me-ChGS-Me thin film structures is explained by sharp increase of the density of the photocurrent in the illuminated portions of the specimen and a strong heating of the ChGS up to the T_g temperature. As a result the viscous forces in the illuminated areas are relaxed and under the action of the electrostatic forces the optical properties (reflectance and transmission) of the recording structure are changed yielding the effect of an optical image recording. Because the deformed grains lie strictly along the illuminated bands of the interference picture, we may also record the holographic information.

The structure of recording media based on Me-ChGS-Me structures and the setup of the recording procedure are shown in the Fig. 15. The microholograms were registered on the recording structures by means of interference of two He-Ne laser beams (1) ($\lambda=6328$ nm) with a power of 10 mW when the electric field (2) is applied. As recording media we have elaborated new

Me-ChGS-Al structures and heterostructures based on amorphous thin films. The latter are more effective, because it exhibits low conductivity in darkness and high photoconductivity due to barrier effects and has a larger spectral sensitivity range as compared with single layer structures.

The proposed recording structure consists of a transparent isolator substrate (3) (glass or polymer), first semitransparent electrode (4) (ITO, SnO_2 , In_2O_3), the photosensitive layer from an amorphous chalcogenide semiconductor (5) (As_2Se_3 , AsSe, etc., or a heterostructure such as $\text{InP}/\text{As}_2\text{Se}_3$, $\text{GaP}/\text{As}_2\text{Se}_3$, $\text{Si}/\text{As}_2\text{Se}_3$, $\text{Ge}/\text{As}_2\text{Se}_3$, $\text{Sb}_2\text{Se}_3/\text{As}_2\text{Se}_3$, $\text{TlSbSe}_2/\text{As}_2\text{Se}_3$, $\text{In}_2\text{S}_3/\text{As}_2\text{Se}_3$, $\text{In}_2\text{Se}_3/\text{As}_2\text{Se}_3$, $\text{Se}/\text{As}_2\text{Se}_3$, etc.), and the second top semitransparent electrode (6) from Al, Au, Sn, Ni, etc. The sensitivity of the recording structures and the diffraction efficiency of elementary holograms depend on the strength and polarity of the electric field, light intensity, electrode material and density of the recorded information. A considerable increase of the diffraction efficiency and sensibility has been reached in the experiments when a series of the applied field pulses of different polarity were applied to the recording structure. The increase of the recording rate when the polarity of the applied field is switched (t_{sw}) leads to the general growth of the sensitivity up to $S = 5 \times 10^3 \text{ cm}^2/\text{J}$ and of the diffraction efficiency up to $\eta = 6 \%$ as a result of an additional electrostimulated chemical interaction of the top Al-electrode with the As_2Se_3 thin film. (Fig. 16). Proposed recording media permits the control and monitoring of the holographic parameters during the recording process. New holographic information technologies for creating data banks and information storage systems of a constant type with high and superhigh capacity based on holographic memory modules and devices compatible with PC was proposed. The software for an automation system of holographic memory by "page to page" reading and handling of binary information from the holographic carrier with a mobile plan was developed [39,40].

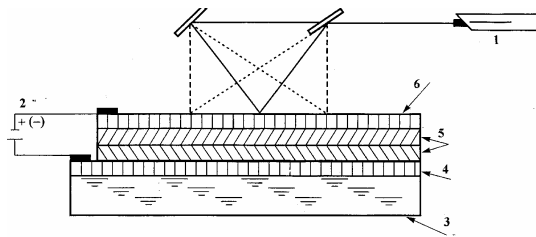


Fig. 15. The structure of the thin film electro-controlled registration media. 1-He-Ne laser; 2-the voltage source; 3-the dielectric substrate; 4-the 1-st transparent electrode (ITO, SnO_2 , In_2O_3); 5-the photosensitive layer from ChGS or heterostructure; 6 - the top transparent electrode (Al, Au, Sn, etc.).

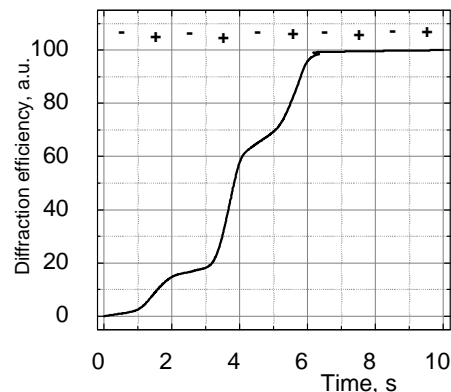


Fig. 6. The kinetics of the diffraction efficiency of microholograms recorded on the Al- $\text{In}_2\text{S}_3/\text{As}_2\text{Se}_3$ -Al heterostructure ($L=0.3/1.0 \mu\text{m}$) when a series of negative and positive ("-" and "+" in the figure) voltage pulses is applied.

Table 2. The parameters of the holographic recording structures.

1.	Spatial resolution	$> 1000 \text{ mm}^{-1}$
2.	Recording wavelength	$0.48 \div 0.63 \mu\text{m}$
3.	Reading wavelength	$0.63 \div 0.87 \mu\text{m}$
4.	Writing time	$40 \div 100 \text{ ms}$
5.	Diffraction efficiency	$5 \div 6 \%$
6.	Sensibility	$6 \times 10^3 \text{ cm}^2/\text{J}$
7.	Storage time	unlimited
8.	Size of one hologram	0.8 mm
9.	Capacity of one hologram	5000 bits
10.	Processor speed (R-R type operation)	$6 \times 10^5 \text{ op/s}$

5.2. High resolution solid state image devices based on the Me-ChGS-SiO₂-Si structures

The optoelectronic methods for processing of information in form of the images, holograms and bits are of great interest for application in the development of the new generation equipment of computers with a great processing speed of the information and in other fields of techniques, such as TV etc. The reversible optoelectronic devices based on metal(Me)-chalcogenide glass semiconductors(ChGS)-dielectric(D)-semiconductor(S)- (ChGSDS) structures were developed and used for writing and readout of the optical images, as a new type sensor of radiation in wide range of energy, and as X-ray solid state image devices [41-43]. The ChGS thin films possessing properties such as high sensitivity, low conductivity, wide range of spectral sensitivity, homogeneity, and high resolution are promising for applications as active elements for optoelectronic processing of the information.

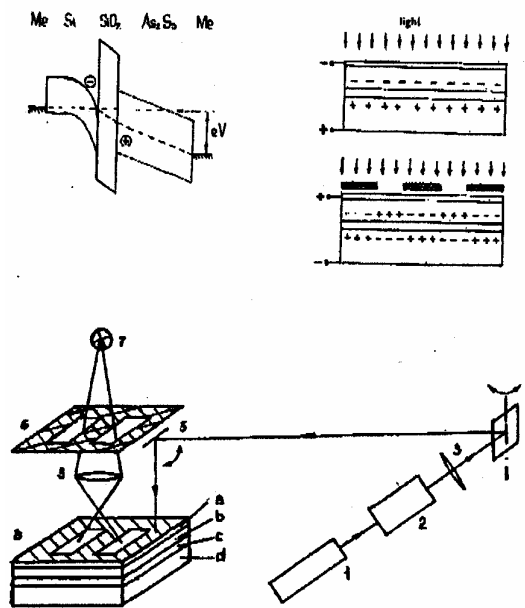


Fig. 17. The schematic energy-band diagram of Me-ChGDS structure during the positive charge writing process and the scheme of writing and readout of the image.

1. He-Ne laser ($\lambda=0.6328 \mu\text{m}$); 2. Modulator; 3. Condensers; 4. 1-st galvanometer mirror;
5. 2-nd galvanometer mirror; 6. The object; 7. Source of illumination; 8. Me-ChDS structure. a) Semitransparent Al-electrode; b) As₂S₃(As₂Se₃) layer; c) SiO₂ layer; d) Si wafer.

The semiconductor structures Me-As₂S₃-SiO₂-Si, Me-As₂S₃:Sn-SiO₂-Si, Me-As₂Se₃-SiO₂-Si, Me-As₂Se₃:Sn-SiO₂-Si were used for writing and readout processes of the optical images with high resolution. The above mentioned structures make the positive and negative images possible. The devices work in both regimes of accumulation of the small signal and real time. There was found that the quantity of accumulated charge versus light intensity have a linear dependence $Q = Q_{max}(\alpha + \beta D)$, where $D = I \cdot t$ - is the dose of radiation. There were studied and developed the signal recording by measuring to the photo-e.m.f., displacement photocurrents and accumulated charge, which allow to propose various type of radiation sensors. The space functional separation of the recording and readout allows to carry out repeated readout of the image without damage and other operations (Fig. 17).

5.3. Variable fiber-optic attenuator controlled by light

Photoinduced phenomena in chalcogenide glass fibers were utilized in order to propose a novel type of variable fiber optic attenuator (VFOA) [44]. It can be used in visible and near IR range of spectrum for continuous change of light intensity in fiber optic circuits. If the lateral surface of ChGS fiber is illuminated by light with photon energy near the glass bandgap a strong decrease of light at the output end of the fiber occurs by changing the optical signal from its initial value I_0 (in the dark) to a new one $I = I_0 \exp(\Delta\alpha L)$, where L is the length of the illuminated segment of the fiber and $\Delta\alpha$ is the PA coefficient. The proposed fiber optic attenuator provides the attenuation in the range 0-20 dB in the 0.8 – 1.8 μm wavelength range. The model of such devices and some parameters are shown in the Fig.18. The construction of the VFOA is miniature and has no moving parts. The attenuator is polarization insensitive and is made in all-fiber technology. The source of illumination can be either W-filament lamps or LEDs.

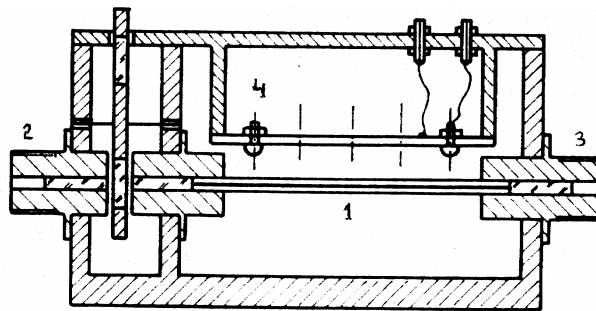


Fig. 18. The model of VFOA.

Specifications:

- Wavelength range (As-Ge-Se fiber)	NIR (0.8-1.8 μm)
- Safe energy level	1 kW/cm^2 CW
- Aperture (green-lens)	\varnothing 1.5 mm
- Attenuation range	\sim 20 dB
- Attenuation resolution	\sim 1 dB
- Insertion loss (without AR coating)	40 %
- Polarization light	non-polarized
- Time change of attenuation coefficient	\sim 3 s
- Dimensions	5 \times 2 \times 2 cm^2
- Weight	\sim 30 g

5.4. Passive and active elements for integrated optics

ChGS thin films are promising materials for the integrated optic devices such as lenses, gratings, optical filters, multiplexors and demultiplexors, optical scanners and printer heads, multiple-output logical elements etc. [21]. A wide variety of light-induced and electron beam changes in ChGS allow fabricate on basis of these effects planar and three-dimensional optical waveguides as well as gratings for integrated optics. An efficiency more than 70 % was demonstrated for the holographic [45] and by electron beam [46] waveguide gratings, for an integrated optical spectral demultiplexor, and for two wavelengths $\lambda_1=630$ nm and $\lambda_2=1150$ nm of a He-Ne laser. Electron-stimulated formation of a relief superimposed diffraction gratings in ChGS amorphous films by electron beam were, also, fabricated [47]. The channel waveguides in amorphous As_2S_3 thin films were obtained using a focused CO_2 ($\lambda=10.6$ μm) laser beam irradiation (Fig. b). It was demonstrated that the value of the refractive index is higher in the annealed region of As_2S_3 [45].

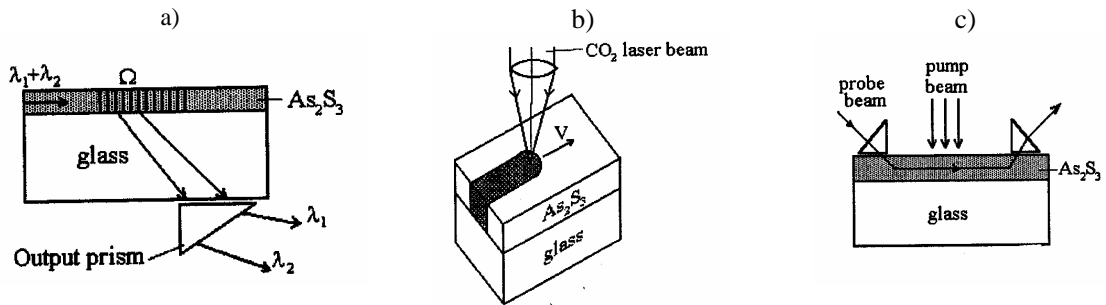
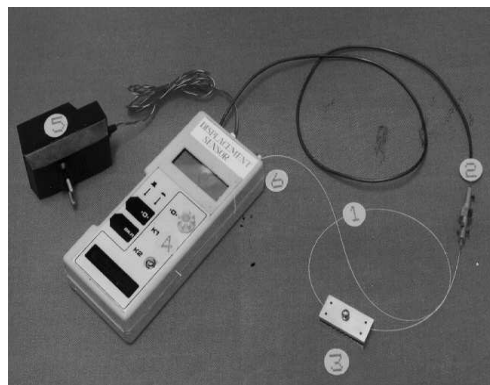


Fig.20. Elements for integrated optics based on ChGS planar waveguides. a) Waveguides gratings for spectral demultiplexing devices; b) Channel waveguides obtained by laser annealing; c) Light-modulator of waveguide beam.

5.5. Fiber optic displacement sensor based on clad modes detection.

Fiber-optic technology offers the possibility for the development of physical sensors for measuring of a wide range of physical parameters. We have developed a microbend displacement sensor with high sensitivity and wide dynamic range designed on the basis of multimode sensor-oriented optical fiber [49,50,51]. The picture and some characteristics of such sensor are shown on Figure below. The sensor consists of a silica step index multimode optical fiber and a conventional deformer. The deformer represents two grooved plates with five teeth. One plate of the deformer can be displaced relatively to the other by a manually adjusting differential micrometer or by means of a piezoelectric transducer. The silica fiber has a modified sensor oriented structure. The sensing section of the fiber represents a short segment which has the coating jacket removed. Instead of the coating jacket a thin film of ChGS is deposited. The deformer is applied on the section of the fiber which is coated with ChGS film. The signal, that is light in the clad modes, was detected by photodiode placed in an integrating sphere. Optical power in the fiber clad is attenuated in propagation to the displacement amplitude via coupling from propagation to radiation modes.



SPECIFICATIONS:

- The range of measured displacements $0 \div 100 \mu\text{m}$;
- The linear range of characteristics $10 \div 60 \mu\text{m}$;
- Deviation from linearity 7 %;
- Sensitivity $0.1 \text{ mV}/\mu\text{m}$;
- Dynamic range 55 dB;
- Insertion losses 16 dB.

1 - Multimode Optical Fiber; 2 - Light Source; 3 - Deformer;
4 - Electronics Package; 5 - Power Supply; 6 - Photodetector.

The sensor is simple in alignment with the light source, has a wide dynamic range and high sensitivity. In addition to displacement such sensor can be modified to detect pressure, acceleration, etc. The described fiber-optic sensor also can be provided with outside acoustic membrane, and thus it can react to changes of temperature and pressure in the ambient medium [52].

References

- [1] G. Lucovsky, *Physical Review* **B6** 1460 (1972).
- [2] G. B. Fisher, Y. Tauc, *Proceed. 5-th Int. Conf. on Amorph. and Liquid Semiconductors*, Ed. by I. Stuke and W. Brenig, Taylor & Francis, London, 1259 (1974).
- [3] M. Popescu, H. Stotzel, L. Vescan, *Proceed. Int. Conf. on Amorphous Semiconductors'80*, **1**, 44, Chisinau (1980).
- [4] J. C. Phillips, *J. Non-Cryst. Solids* **34**, 53 (1979).
- [5] G. Lucovsky, F. L. Galeener, *J. Non-Cryst. Solids* **37**, 53 (1980).
- [6] M. S. Iovu, S. D. Shutov, M. Popescu, D. Furniss, L. Kukkonen, A. B. Seddon, *J. of Optoelectronics and Advanced Materials* **2**, 15 (1999).
- [7] N. Mott, E. A. Davis, *Electronic Processes in Non-Crystalline Materials*, M., Mir (1974) (Rus).
- [8] A. I. Gubanov, *Quantum Electron Theory of Amorphous Semiconductors*, M.-L., Nauka (1963) (Rus).
- [9] M. H. Cohen, H. Fritzsche, S. R. Ovshinsky, *Phys. Rev. Letters* **22**, 1065 (1969).
- [10] B. T. Kolomiets, *Proceed. 19-th Int. Conf. on Physics of Semiconductors*, M.-L., Nauka, 1335 (1969) (Rus).
- [11] J. M. Marshall, A. E. Owen, *Phil. Mag.* **24**, 1281 (1971).
- [12] V. L. Bonch-Bruевич, *JETF* **61**, 1168 (1971).
- [13] R. A. Street, N. F. Mott, *Phys. Rev. Letters* **35**, 1293 (1975).
- [14] A. M. Andriesh, S. A. Malkov, V. I. Verlan, N. A. Gumeniuk, *Phys. Stat. Sol.(b)* **163**, K39 (1991).
- [15] S. D. Shutov, A. A. Simashchevich, *J. Non-Cryst. Solids* **176**, 253 (1994).
- [16] G. Pfister, A. Scher, *Advances in Physics* **27**, 747 (1978).
- [17] V. I. Arkhipov, M. S. Iovu, A. I. Rudenko, S. D. Shutov, *Phys. Stat. Sol. (a)* **54**, 67 (1979).
- [18] M. S. Iovu, M. G. Bulgaru, S. D. Shutov, *Balkan Phys. Letters* **4**, 147 (1996).
- [19] A. M. Andriesh, in "Physics and Application of Non-Crystalline Semiconductors in Optoelectronics", Kluwer Academic Publications, Dordrecht/Boston/London, p.17, (1997).
- [20] B. P. Antonyuk, S. A. Kisilev, M. Bertolotto, C. Sibilia, G. Leakhov, A. M. Andriesh, *Phys. Rev.* **B47**, 10186 (1993).
- [21] M. Popescu, A. Andriesh, V. Ciunash, M. Iovu, S. Shutov, D. Tsiuleanu, *Fizica Sticlelor Calcogenice (roum.)*, Ed. Stiintifica Bucuresti-I. E. P. Stiinta Chisinau (1996).
- [22] E. Busse, S. R. Nagels, *Phys. Rev. Letters* **47**, 1848 (1981).
- [23] M. S. Iovu, S. D. Shutov, A. M. Andriesh, E. I. Kamitsos, C. P. E. Varsamis, D. Furniss, A. B. Seddon, M. Popescu, *J. of Optoelectronics and Advanced Materials* **3**, 443 (2001).
- [24] A. Ganjoo, N. Yoshida, K. Shimakawa. *Recent Research Developments in Applied Physics*, ed. M. Kawasaki, N. Ashgritz, R. Anthony (Research Signpost, Trivandrum, **2**, 129 (1999).
- [25] M. Iovu, S. Shutov, S. Rebeja, E. Colomeycu, M. Popescu, *J. of Optoelectronics and Advanced Materials* **2**, 53 (2000).
- [26] A. M. Andriesh, I. P. Culeac, V. M. Ioghin, *Pure and Applied Optics* **1**, 91 (1992).
- [27] A. M. Andriesh, I. P. Culeac, P. J. S. Ewen, A. E. Owen, *J. of Optoelectronics and Advanced Materials* **3**, 27 (2001).
- [28] S. R. Ovshinsky, *Proceed. 20-th Int. Semicond. Conf. CAS'97, Sinaia, Romania* (1997), p. 33.
- [29] N. Yoshida, M. Itoh, K. Tanaka, *J. Non-Cryst. Solids* **198-200**, 749 (1996).
- [30] N. Yoshida, K. Tanaka, *J. Non-Cryst. Solids* **210**, 119 (1997).
- [31] M. Popescu, F. Sava, A. Lorinczi, E. Scordeva, P. Y. Koch, H. Bradaczek, *Proceed. 20-th Int. Semicond. Conf. CAS'97, Sinaia, Romania* (1997), p. 27.
- [32] M. Popescu, M. Iovu, W. Hoyer, O. Shpotyuk, F. Sava, A. Lorinczi, *J. of Optoelectronics and Advanced Materials* **3**, 303 (2001).

- [33] A. Andriesh, V. Chumash, *Pure and Applied Optics* **7**, 351 (1998)
- [34] S. R. Ovshinsky, in: *HOMAGE BOOK* dedicated to Acad. A. Andriesh, Ed. by M. Popescu, INOE&INFM Publishing House, Bucharest-Romania (1999), p.15.
- [35] A. M. Andriesh, S. D. Shutov, D. I. Tsiuleanu, *Sposob Zapisi Informatsii na besserebreanih nositelei*, Naukova Dumka, Kiev, **7**, 55 (1976).
- [36] A. M. Andriesh, V. V. Bivol, A. I. Buzdugan, M. S. Iovu, L. M. Panasyk, G. M. Triduh, V. I. Fulga, D. I. Tsiuleanu, S. D. Shutov. *Stecloobraznye Poluprovodnichi v Photoelectriceskikh Sistemah Zapisi Opticeschoi Informatsii*, Ed. By A. M. Andriesh, Stiintsa Press, Chisinau (1984).
- [37] A. M. Andriesh, M. S. Iovu, V. V. Bivol, E. G. Khanchevskaya, *Optical Memory and Neural Networks* **4**, 69 (1995).
- [38] A. M. Andriesh, E. A. Akhimova, V. V. Bivol, E. G. Khancevskaya, M. S. Iovu, S. A. Malkov, V. I. Verlan, *Int. J. of Electronics* **17**, 339 (1994).
- [39] V. Bivol, A. Andriesh, M. Iovu, A. Prisacari, *Proceedings of the 5-th International Symposium for Design and Technology of Electronic Modules SIITME'99*, Sept. 23-26, 1999, IEEE, Bucharest, Romania, 110 (1999).
- [40] V. Bivol, T. Necsoiu, *Proceedings of the 6-th International Symposium for Design and Technology of Electronic Modules SIITME'2000*, Sept. 21-24, 2000, IEEE, Bucharest, Romania (2000), p.116.
- [41] A. M. Andriesh, V. I. Verlan, S. A. Malkov, In: *High Resolution Cameras and Recording Devices and Laser Scanning and Recording Systems*, Ed. By L. Beiser and R. Lenz, **1987**, 171 (1993).
- [42] A. M. Andriesh, S. A. Malkov, V. I. Verlan, *Optoelectronica*, Bucharest, 1994, p.4.
- [43] A. M. Andriesh, S. A. Malkov, V. I. Verlan. In: *Solid State Sensor Arrays: Development and Application Conference, IST/SPIE Symposium on Electronic Imaging: Science, Technology*, Jan. 1996, San-Jose, USA, p.153.
- [44] A. Andrieh, I. Culeac, V. Binkevich, V. Abashkin, T. Necsoiu, S. Miclos, A. Aiftimei, *Abstr. 4th Symposium of Optoelectronics SIOEL'96*, Sept. 18-20, Bucharest, Romania, 1996, p.7.
- [45] A. Popescu, in: *HOMAGE BOOK* dedicated to Acad. A. Andriesh, Ed. by M. Popescu, INOE & INFM Publishing House, Bucharest-Romania (1999), p.211.
- [46] S. A. Sergeev, S. D. Shutov, *Romanian J. of Optoelectronics* **5**, 32 (1997)
- [47] S. A. Sergeev, S. D. Shutov, *Surface Engineering and Applied Electro-Chemistry* **6**, p.41, U.S.A. (1995).
- [48] R. Radvan, R. Savastru, D. Ghica, V. Bivol, A. Prisacari, G. Triduh, In "Physics and Applications of Non-Crystalline Semiconductors in Optoelectronics", Ed. by A. Andriesh and M. Bertolotti, Kluwer Publishers, NATO ASI Series. 3. High Technology, v.36, p.17 (1997).
- [49] A. M. Andriesh, I. P. Culeac, V. A. Bechevich, V. G. Abashchin, V. N. Scitsco, *Letters of Academy of Sciences of Moldova, Fizica & Tehnica* **3**, 3 (1993).
- [50] A. Andriesh, V. Abaskin, V. Binkevici, I. Culeac, V. Schitsko, V. Necsoiu, A. Aiftimei, S. Miclos, T. Zisu, *Optoelectronica* **4**, p.16 (1996).
- [51] A. Andriesh, I. Culeac, V. Abashkin, V. Binchevici, *Romanian J. of Optoelectronics* **5**, p.129 (1997).
- [52] V. Bivol, V. Abashkin, C. Cotirlan, *Abstr. 5-th Symposium of Optoelectronics SIOEL'98*, Sept. 23-25, Bucharest, Romania, p.61, 1998.